

Research Article

Received on: 28-04-2018

Accepted on: 03-05-2018

Published on: 10-05-2018

Corresponding Author:

***Irina Kadiyala**
Pharmaceutical and
Preclinical Sciences
Vertex Pharmaceuticals
Boston, MA 02210
USA
Phone No.: +1 617-341-6100

Mechanical Characterization of Extracellular Matrix Hydrogels: Comparison of Properties Measured by Rheometer and Texture Analyzer

Taraka Sai Pavan Grandhi, Noreen Zaman, Alamelu Banda, Varsha Dhamankar, Cathy Chu, Emily Perotta, Irina Kadiyala*

ABSTRACT

Extracellular matrix (ECM) hydrogels have shown remarkable benefit as new materials for regenerative medicine for multiple applications. However, for ECM-based materials to be used in vivo, they must possess appropriate mechanical properties to enable handling during storage and administration, as well as properties to induce the needed biological responses. The experiments carried out in this study allowed deeper understanding of the physical characteristics of gels towards their use in a clinical setting and subsequent commercialization. Using rheometer and texture analyzer, we expanded the previously reported mechanical characterization of ECM gels and here we present data on the new tests such as constant shear at different temperatures; cross-over temperature/gel point; cohesivity, adhesivity and hardness; fitting to Burger's model; and strain-stiffening. We compared the mechanical properties of ECM hydrogels to collagen hydrogels, the latter were used as an internal control. Mechanical properties of ECM hydrogels were measured during different stages of hydrogel formation (pre-gel, gelation and formed hydrogel). Overall, gel complex modulus measured using rheometer correlated with hardness measured using texture analyzer across measured hydrogel concentrations, indicating that the measurements



*Email Id
irina_kadiyala@vrtx.com

Cite this article as:

Taraka Sai Pavan Grandhi, Noreen Zaman, Alamelu Banda, Varsha Dhamankar, Cathy Chu, Emily Perotta, Irina Kadiyala, Mechanical Characterization of Extracellular Matrix Hydrogels: Comparison of Properties Measured by Rheometer and Texture Analyzer, 6(28); 11-20, 2018. www.asianpharmtech.com

Taraka Sai Pavan Grandhi, Harrington Biomedical Engineering, Arizona State University, Tempe, AZ 85281, USA

Noreen Zaman, Pharmaceutical and Preclinical Sciences, Vertex Pharmaceuticals Incorporated, Boston, MA 02210, USA

Alamelu Banda, Pharmaceutical and Preclinical Sciences, Vertex Pharmaceuticals Incorporated, Presently at Genentech, San Francisco CA, 94080, USA

Varsha Dhamankar, Pharmaceutical and Preclinical Sciences, Vertex Pharmaceuticals Incorporated, Boston, MA 02210, USA

Cathy Chu, Pharmaceutical and Preclinical Sciences, Vertex Pharmaceuticals Incorporated, Boston, MA 02210, USA

Emily Perotta, Pharmaceutical and Preclinical Sciences, Vertex Pharmaceuticals Incorporated, Boston, MA 02210, USA

done with rheometer and texture analyzer were complementary to each other. In addition, two model drugs with poor solubility and similar molecular weight, but differing in charge were incorporated into the UBM ECM hydrogel to study the rheological behavior of the drug-hydrogel composites. The presence and properties of the drugs were found to have a moderate effect on hydrogel mechanical properties depending on the charge of the drug.

Key-words: Extracellular matrix (ECM) hydrogels, Rheometer, Texture analyzer

INTRODUCTION

Hydrogels are formed from hydrophilic, water insoluble polymeric matrices that swell under aqueous conditions (1) and exhibit a wide range of mechanical properties. They have been shown to be safe and biocompatible, and have generated much interest in the burgeoning field of regenerative medicine (2). Unlike polymerizing systems that require the addition of external catalysts, copolymerizing agents or photo polymerizing compounds to initiate gelation, some naturally occurring gels can undergo rapid physical gelation upon a change in environmental conditions. Thermosensitive hydrogels, which include naturally occurring hydrogels composed of collagen or extracellular matrix (ECM), undergo phase transition from liquid to solid in response to a change in temperature, and have drawn particular interest due to their vast potential applications. These hydrogels are thermoplastic and can be injected as liquids via commonly used gauge needles at an injury site; an increase in temperature to 37°C will cause them to gel in-situ, thus making them a valuable tool for minimally invasive drug delivery (3-5).

Whole ECM gels consist of a complex mixture of glycosaminoglycans (GAGs), non-structural proteins and structural proteins such as collagen, fibronectin, laminin and elastin, each of which has shown some regenerative capacity (6-9). ECM gels are gaining traction in research and the clinic due to their higher regeneration potential, e.g. for CNS regeneration (10-13). ECM gels promote regeneration by recruitment of endogenous stem and progenitor stem cells from the surrounding tissues (14). Soluble proteins in the ECM matrix create a chemotactic gradient for the stem cells to migrate, whereas insoluble proteins provide a structural and mechanical framework for the cells to differentiate upon (14). ECM gels characterized in this study were derived from porcine urinary bladder (UBM ECM) and have shown immense benefit in tissue regeneration in multiple animal models, pre-clinical trials and small human clinical studies (15-18). In addition to providing chemical signals, the mechanical properties of the hydrogels have been found to be important in regulating the biological responses (5,19,20). For example, materials with elastic modulus of about 0.5 MPa have been shown to stimulate neuronal stem cells to mature into neurons for regeneration (21,22) and be used for the treatment of stroke (23). Or ECM gels with elastic stiffness of 0.4-0.9 MPa have been shown to have varying regenerative capacity in the liver depending on formulation composition (24).

In-depth understanding of hydrogel mechanical properties can aid in the optimization of hydrogel preparation and improve their administration in the clinic. While ECM hydrogel viscoelastic properties by rheology have been published previously in multiple papers (5,6,25), we expanded our understanding of the mechanical properties using novel techniques such as constant shear at different temperatures, cross-over temperature or gel point, cohesivity, adhesivity, and hardness, and strain-stiffening. In addition, while there are studies showing the use of rheometer (25) and limited studies showing the use of texture analyzer for mechanical characterization of ECM hydrogels (yield stress, strain, gelation kinetics, etc.) (6), there are no studies providing a direct comparison between the characterization by rheometer and texture analyzer. We present procedures for characterization of UBM ECM hydrogels using these two instruments that offer complementary data and tools. Multiple rheological and texture properties of the hydrogel were measured under surface-parallel shear forces and normal forces respectively. Furthermore, ECM hydrogel results from both techniques (rheological and texture based) were compared to that of collagen gels, which have been used extensively by other researchers and provide an internal reference. In addition, we determined the impact of drug loading on the mechanical properties of the ECM drug-hydrogel composite using two model drugs, glipizide and tamsulosin, and identified properties of the drugs that may impact gel formation. Incorporation of drugs into the hydrogel can provide additional therapeutic benefit when administered at the site of injury. The work presented here might provide a platform for the study of UBM ECM, collagen or novel hydrogels for therapeutic use.

EXPERIMENTAL SECTION

Materials

Powdered urinary bladder matrix (UBM) was provided by the Stephen Badylak Laboratory, McGowan Institute of Regenerative Medicine, University of Pittsburgh (Pittsburgh, PA, USA). FibrilCol Bovine Collagen, Type I (10 mg/mL) was obtained from Advanced BioMatrix (Carlsbad, CA, USA). Pepsin, Pluronic F127 and glipizide were obtained from Sigma-Aldrich (St. Louis, MO, USA). Tamsulosin was obtained from Selleck Chemicals (Houston, TX, USA). 10x phosphate buffered saline (PBS) was prepared in-house at Vertex Pharmaceuticals and diluted to 1x PBS with water. Nanopure water was used for all preparations unless specified. Stress controlled Discovery Hybrid Rheometer-1 from TA instruments (New Castle, DE, USA) was used in rheological measurements. The TA.XTPlus Texture Analyzer (Stable Micro Systems, Godalming, UK) was used for texture analysis.

Preparation of UBM ECM and Collagen Pre-Gel Solutions

Detailed description of ECM pre-gel solution preparation is presented in Freytes et al. (6). In brief, 100 mg of lyophilized UBM ECM powder was mixed with 10 mg of pepsin in 10 mL of 0.01 N HCl for 48 h at room temperature. The pre-gel solution was prepared by an acid neutralization method. The stock solution was diluted with 1X PBS and neutralized with 0.1 N NaOH to pH 7.2-7.4. Collagen pre-gels were also prepared by acid neutralization with 0.1 N NaOH and 1x PBS as per the protocol of the vendor (Advanced BioMatrix) (26). UBM ECM gel and collagen gels were prepared at 2, 4 and 8 mg/mL for rheological and texture analyzer characterization described below.

Two small molecule model drugs (glipizide and tamsulosin) sparingly soluble in water were incorporated into the UBM ECM gels. The chosen drugs have similar molecular weight (~400 Da) and logP (~2.8), but vary in charge. Glipizide is negative at neutral pH, and tamsulosin is positive at neutral pH. These drugs were incorporated into 4 mg/mL UBM ECM hydrogels at 25 and 50 wt%/wt%. To eliminate the potential effect due to differences in particle size, the drugs were screened and a particle size fraction of 106 to 212 μm was used for these experiments for both drugs. Each drug (25 or 50% by total weight) was mixed with Pluronic F127 (6.25% by total weight) and the drug/Pluronic F127 mixture was subsequently combined with the UBM ECM stock solution (4 mg/mL). The drug-ECM pre-gel mixture was then neutralized as described above.

Methods

Figure 1 details the various characterizations carried out at the different phases of gel formation and specifies the instrument used for the respective measurements. For all rheometer tests, measurements were initiated by adding 800 μL of pre-gel solution to the plate and cone (1.995°) geometry on the TA Instruments DHR-1 series rheometer. The bottom plate of the rheometer was maintained at 4°C until the start of the experiment. The vendor guidelines were followed for various experiments that were carried out unless specified (27). Gel and hydrogel terminology are used interchangeably. All terminology used in this study is consistent with the TA manual (27).

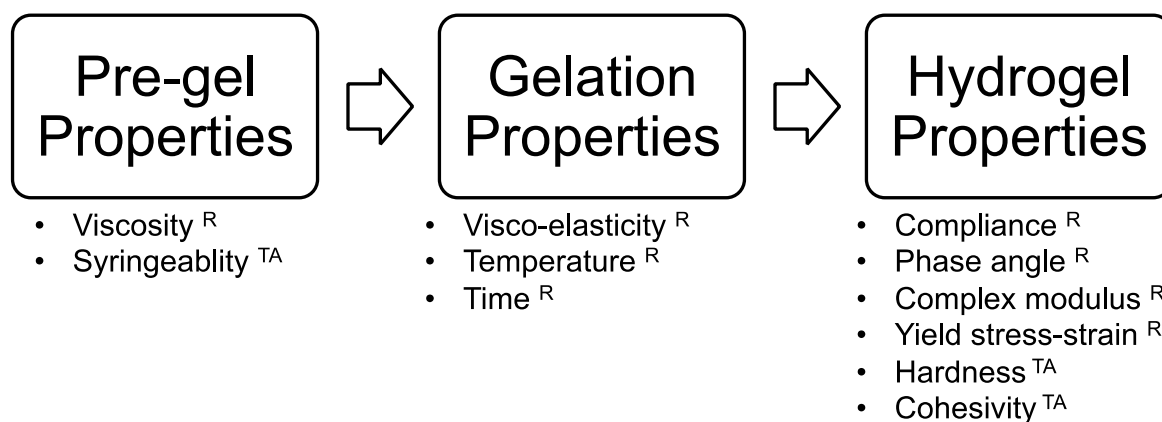


Figure 1. Description of characterization conducted for each of the hydrogel stages. Experiment conducted on: R=Rheometer, TA=Texture Analyzer

Pre-gel solution properties

The UBM ECM and collagen pre-gel solutions were characterized by rheometer for viscosity, and by texture analyzer for syringeability.

Viscosity: The viscosity of the pre-gel solutions was determined by constant shear and shear ramp methods. For constant shear measurements, the viscosity was measured at 4°C and 10°C at 1 Pa shear for 5 min. For shear ramp measurements, the pre-gels were subjected to a shear ramp from 1-1000 1/s. The shear ramping experiment was conducted at 4°C since the pre-gel solution gels at the higher temperatures. The Herschel-Bulkley equation was fitted to the data to determine flow indices.

Syringeability: Syringeability (resistance to extrusion) was measured on the UBM ECM and collagen pre-gel solutions. Syringeability was measured by applying a normal force on the syringe piston using a flat probe connected to the TA.XTPlus instrument. Approximately 0.5 mL of solution was extruded from a 1½" 21G needle with a 1mL syringe at a rate of 1 mm/s. The mean force produced was recorded with a detection limit set at 0.5 g of force.

Gelation properties

The gel point and temperature-responsiveness of the materials were determined on the rheometer.

Gel Point: The time required for gelation, which is defined as the gel point, was measured by tracking the storage modulus (G') of the gel. The gelation process was studied for the UBM ECM and collagen gels on the rheometer using two methods. In the first method (flash method), the temperature was increased from 4°C to 37°C in less than one minute after introduction of the pre-gel to the rheometer. The pre-gels were exposed to a strain of 0.1% with a constant angular frequency of 1 rad/s.

Temperature-responsive gelation test: In the second method (ramp method), the pre-gel solutions were exposed to a strain of 0.1% with a constant angular frequency of 1 rad/s while the temperature was gradually ramped from 4°C to 37°C at a rate of 0.33°C/min. The storage modulus (G') and loss modulus (G'') were tracked and the time where $G'=G''$ was determined to be when gelation occurred.

Hydrogel properties

Dynamic mechanical analysis was carried out on the formed UBM ECM and collagen hydrogels on the rheometer to determine the storage, loss and complex moduli, phase angle, yield strain, and yield stress. The hardness, cohesivity and adhesivity of both gels were determined on the texture analyzer.

Dynamic mechanical analysis: Storage modulus (G'), loss modulus (G''), complex modulus (G^*) and phase angle ($\tan \delta$) were measured by applying a strain of 0.1% with an angular frequency of 1 rad/s.

Yield strain was measured by amplitude sweep, which involves applying a strain from 0.001 to 100% at a constant angular frequency of 1 rad/s. A logarithmic exponential decrease in the storage modulus was determined to be the yield strain (%) value.

Yield stress was measured by creep method, which involves applying incremental stress until strain recovery was incomplete. The procedure was as follows. A constant stress of 0.1 Pa was initially provided for 60 s followed by a recovery time of 540 s. The constant stress was ramped up 1.5 fold with each repeat across 20 repeats. Yield stress was measured as the stress value at which the strain (%) after recovery was incomplete and approximately equal to or greater than 0.5% strain.

Burger's model was used to fit the creep data to calculate strain under prolonged stress conditions. Constant stress creep measurements were performed to compare the predicted strain values from the model to the measured values for the rheometer.

Hardness, cohesivity and adhesivity: Approximately 750 μ L UBM ECM or collagen pre-gel solution were cast in 2 mL vials for 90 min at 37°C. The gels were impinged with a cylindrical rod on the TA.XTPlus Texture Analyzer at a rate of 1 mm/s up to a distance of 5 mm into the gel. Force measurement was initiated after reaching the trigger force of 0.5 g. Initial peak of the force time curve was noted as the hardness peak, area under the positive region of the curve as cohesivity and area under the negative region of the curve as adhesivity.

Statistical Analysis

One-way ANOVA was used to compare the different gel properties at three different concentrations. Pairwise comparisons were performed using Tukey's multiple comparisons test (Tukey-Kramer method) to understand the differences between individual concentrations. Significance was defined as $p < 0.05$.

RESULTS AND DISCUSSION

Various hydrogel mechanical properties were measured with rheometer and/or texture analyzer at each step of hydrogel formation (i.e., pre-gel solution, gelation and hydrogel) (Figure 1). Mechanical properties of hydrogels have been shown to influence multiple important biological properties such as adhesion and cell spreading (28), migration (29), proliferation (30) and differentiation (31). In addition to the mentioned biological properties, adequate mechanical properties are necessary for manufacture, ease of handling and administration. The experiments carried out in this study allow understanding of the physical characteristics of gels towards their use in a clinical setting and subsequent commercialization. The characterization results obtained for the UBM ECM hydrogels are presented first, followed by a comparison with collagen hydrogels.

Pre-Gel Properties

Viscosity

Pre-gel solution viscosity is an important material property to determine the ease of on-site administration because solutions with high viscosity present a challenge to administration via an appropriately sized needle. Viscosity was measured by both constant shear and shear ramp methods on the rheometer. The constant shear method provides the response of viscosity to an increase in temperature and concentration, and the shear ramp method provides the response of viscosity to an increase in shear.

As seen from the data (Figure 2a), for the constant shear method at 1 Pa, viscosity significantly increased with concentration but not temperature over the ranges studied. For the shear ramp method, viscosity of the solutions was seen to decrease with increasing shear rate, indicating that the pre-gel solutions were shear thinning or thixotropic (Figure 2b). The ECM pre-gels are mostly complex mixtures of randomly oriented proteins and glycosaminoglycans (GAGs) initially bound together with hydrogen and Van Der Waals interactions that provide resistance to flow at low shear. Higher shear stresses overcome these bonds and cause the proteins and GAGs to align, resulting in shear thinning (Figure 2b) (32).

The data obtained from the shear stress vs. shear rate curve was fitted to the Herschel–Bulkley equation (Equation 1) to determine the flow index, which provides information on the extent of shear thinning. Flow index values suggested that the shear thinning behavior of the ECM pre-gels was more pronounced at higher concentrations.

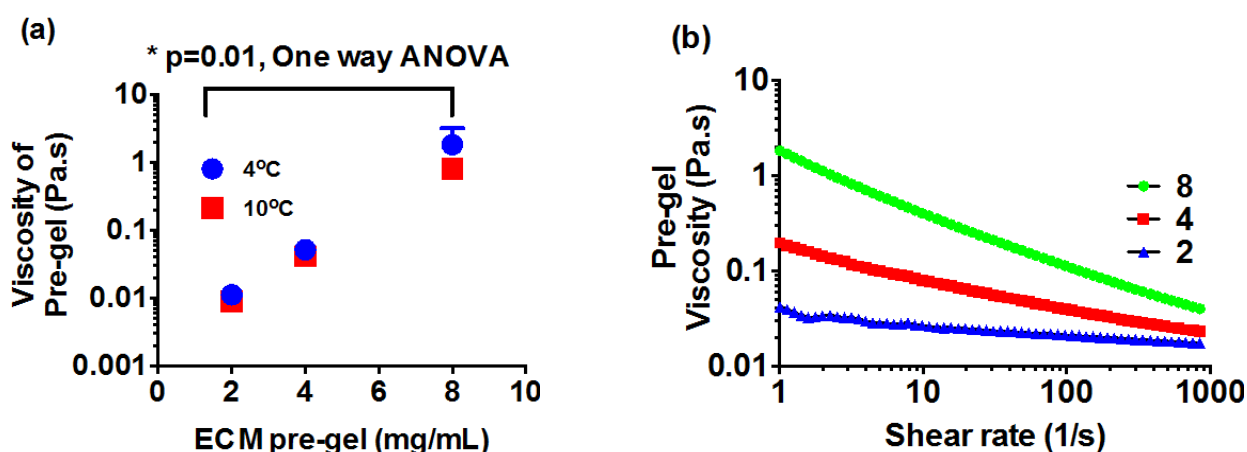


Figure 2. UBM ECM pre-gel solution viscosity measured ($n=3$) for with a) Constant shear of 1 Pa at 4 and 10°C, and b) Shear ramp (1-1000 s^{-1}) at 4°C for 2 (blue), 4 (red) and 8 (green) mg/mL gels. Gels were shown to be thixotropic, with increasing viscosity at higher concentrations.

Herschel-Bulkley equation:

$$\sigma = \sigma_0 + K\dot{\gamma}^n \quad (1)$$

Where K =Consistency index (consistency index provides information on solution viscosity) and n =Flow index.

Table 1 shows the flow index values for ECM pre-gels at 2, 4 and 8 mg/mL concentrations. Newtonian fluids have a flow index of 1, whereas shear-thinning pseudoplastic fluids have a flow index less than 1. As seen in Table 1, the 8 mg/mL pre-gels have the lowest flow index indicating a higher degree of shear thinning. It is likely that a higher concentration of proteins provides a higher degree of shear thinning in the 8 mg/mL ECM gel. The shear thinning property at high shear rates of these pre-gels could be beneficial during their administration due to the reduction in resistance to movement.

Table 1: Flow index of ECM pre-gels measured via shear ramp (n=3). Lower flow index at higher gel concentrations indicate greater extent of shear thinning.

ECM Concentration (mg/mL)	Flow Index (n)
2	0.90
4	0.75
8	0.55

Syringeability

The syringeability force of the ECM pre-gels was compared to a control (D5W) to provide an understanding about the relative ease of administration. The force required to extrude D5W was measured to be about 146 g. As seen in Figure 3, the force required to push the pre-gels out of a 1½" 21G needles was comparable to that of D5W at 4°C indicating equivalent ease of administration of the ECM pre-gel solutions. We conducted this study at 4°C since the gel point was found to be approximately 25°C. Syringeability of ECM pre-gels was found to be independent of concentration, despite significant differences in viscosity (Figure 2a). It is likely that the normal force applied to the syringe piston caused shear thinning of the pre-gel solution upon its extrusion from the needle. Further studies are recommended to justify the diameter for the selected gauge of needle, as well as to optimize the pre-gel handling and administration to prevent its gelling.

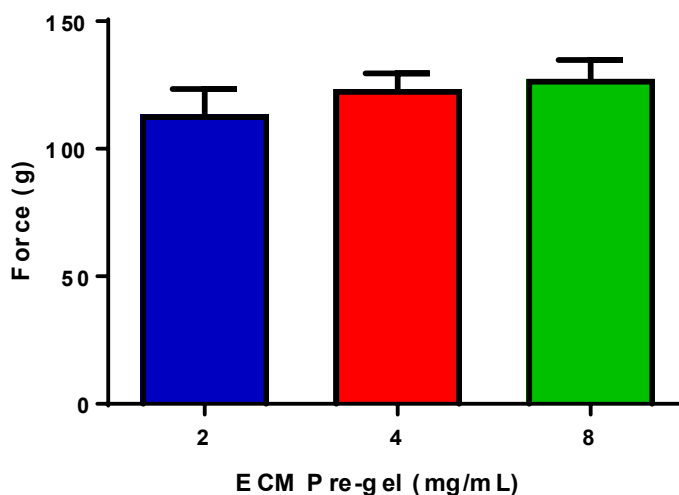


Figure 3. ECM pre-gel solution syringeability at 2, 4 and 8 mg/mL ECM at 4°C (n=3).

Gelation Properties

Gel point

To mimic the conditions in-vivo after injection of pre-gel solution to the body, temperature was flash ramped from 4°C to 37°C (flash gelation) in less than one minute, and gelation kinetics were monitored by tracking the G' and G'' values. Complete gelation was measured by recording the time taken for G' (storage modulus) to reach a plateau (Figure 4a) and occurred within 5 min for all gels. There was no difference observed between the 2,

4 and 8 mg/mL concentration groups (Tukey's multiple comparisons test) (Figure 4b). In the study by Liang et al. (33), a gelation time of 5 min was found to be optimal for microinjection of hyaluronic acid-gelatin hydrogels into spinal cord gray matter of Sprague Dawley (SD) rats.

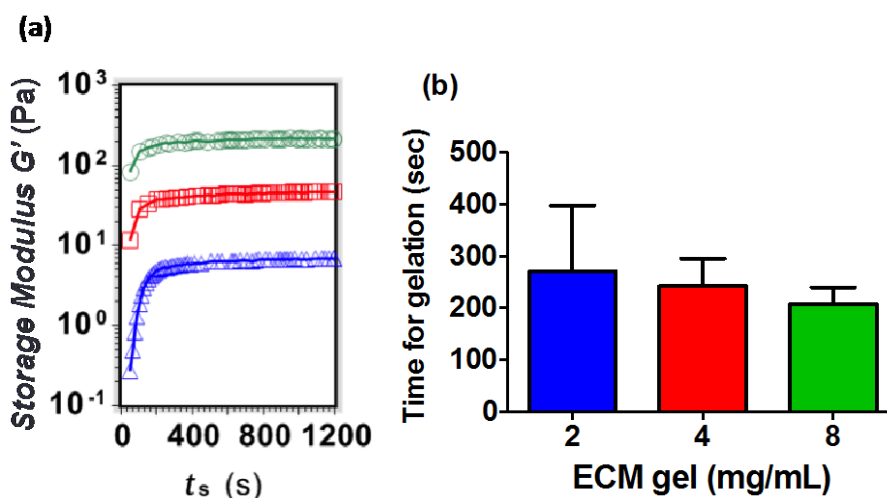


Figure 4. a) Storage modulus during UBM ECM gelation ($n=3$) due to flash temperature increase from 4°C to 37°C. b) Gel point of UBM ECM gels at: 2 mg/mL (blue), 4 mg/mL (red) and 8 mg/mL (green).

It is likely that the unique composition of these ECM hydrogels plays a major role in impacting their gelation kinetics. ECM gels were shown to contain mostly collagen with a complex mixture of other soluble and insoluble proteins (proteoglycans, sulfated GAGs, fibronectin, etc.) (6). It is known that these proteins impact collagen fibrillogenesis and gelation in multiple complex ways. Collagen gelation takes place via a two-step process of lag-phase nucleation where thin filaments are formed, followed by a growth phase marked by fibril growth and interconnections (34,35). Proteoglycans and glycosaminoglycans in the ECM matrix influence the length of both the lag and growth phases of collagen gelation. These components can act as accelerators and decelerators of gelation. Chondroitin sulfate and keratin sulfate accelerate the lag phase, whereas heparin sulfate retards it. On the other hand, chondroitin sulfate delays the growth phase (36). In addition, large proteoglycans/sGAGs can also retard the free diffusion of self-assembling peptides that cause gelation, leading to weaker gels compared to single agent gels (i.e., collagen) (35). It is possible that with an increase in ECM concentration, the concentration of accelerators and decelerators increase equally, thereby having no overall impact on the gelation time. This property could be leveraged to tune the gelation temperature/time of these ECM gels. On the other hand, single agent collagen gel does not express this behavior where a concentration dependent decrease in temperature of gelation has been shown (37).

Temperature-responsiveness of gelation

To assess the temperature-responsiveness of gelation, temperature was increased at a rate of 0.33°C/min from 4°C to 37°C to initiate physical gelation. As can be seen in Figure 5a, the loss modulus (G'' , red) was higher than the storage modulus (G' , blue) before gelation indicating the liquid-like viscous sol state of the pre-gel solution. As temperature increased, G' was seen to rise faster than G'' indicating the increase in the elastic energy stored in the gel as gelation occurred. Gelation occurs when G' is equal to G'' . The gels tested exhibited the cross-over at approximately 25°C (Figure 5b) and the time to gelation (gel point ($G'=G''$)) was independent of concentration (Figure 5c). As seen from Figure 5a, after gelation, the system has higher storage modulus than loss modulus indicating a switch from liquid-like to solid-like state.

Hydrogel Properties

Gel dynamic mechanical analysis, hardness, cohesivity and adhesivity

To assess the mechanical stiffness of the UBM ECM gels phase angle (δ), storage modulus (G') and hardness were measured. Phase angle for all the gels was in the range of ~5-10° (Figure 6a). The elastic regime is 0-90°,

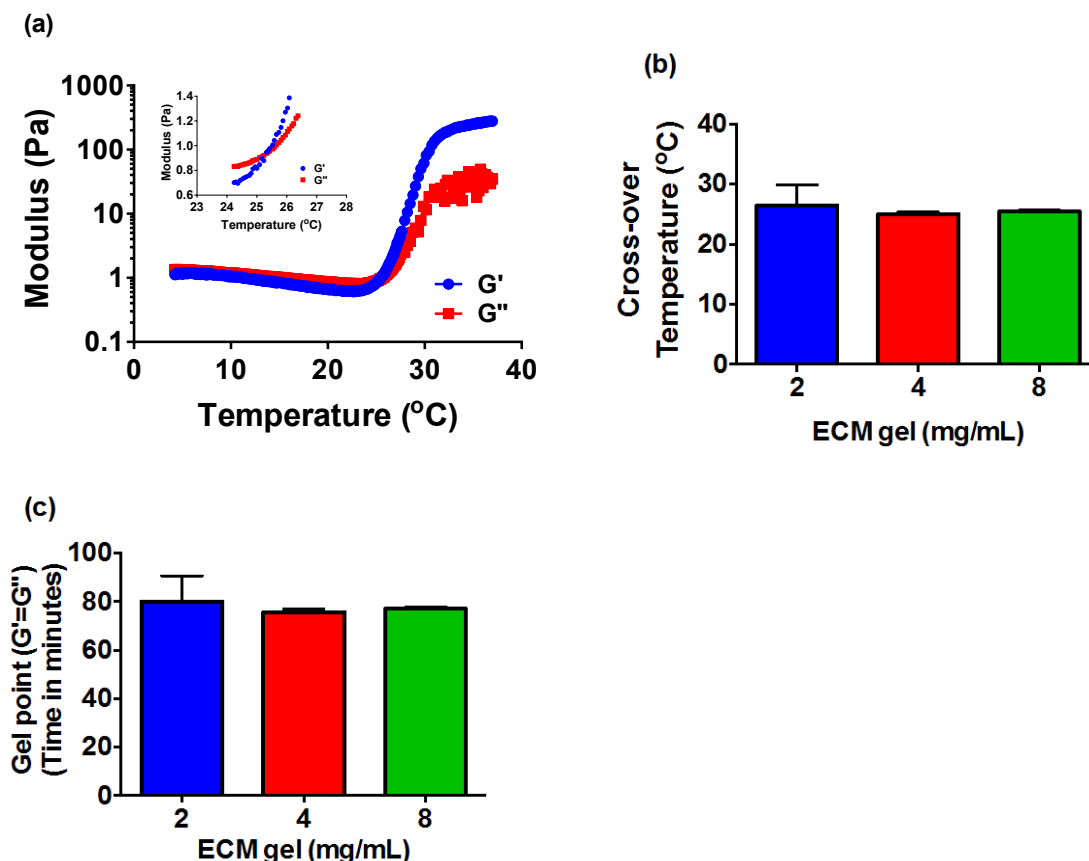


Figure 5. Gelation kinetics (n=3): a) Cross-over temperature during temperature sweep (0.33°C/min). Data for 8 mg/mL ECM gel is shown. b) Cross-over temperatures for 2, 4 and 8 mg/mL gels are shown. c) Cross-over time (gel point $G'=G''$) for 2 (blue), 4 (red) and 8 (green) mg/mL gels is shown.

indicating that gels in this study were predominantly elastic. Both the storage and complex modulus for all gels were in the range of 10-270 Pa (Figure 6b), and showed a concentration dependent increase ($p < 0.001$, one-way ANOVA). In our case, storage and complex moduli are similar due to elastic nature of the ECM material. The stiffness of the UBM ECM gels was similar to the stiffness of brain tissue and thus would be appropriate for neural regeneration. The latter is supported by the study by Saha et al. (22), in which an interpenetrating polymer network of storage modulus 33-167 Pa was shown to differentiate adult neural stem cells into neurons *in vitro*.

While complex modulus measured by rheometer allowed analysis via surface parallel shear forces, texture analyzer allowed measurement of gel performance under surface normal forces, and was used to measure the gel hardness, cohesivity and adhesivity. Like the storage modulus, gel hardness was seen to increase with increasing concentration ($p < 0.001$, one-way ANOVA) (Figure 6c). An increase in gel hardness (measured by texture analyzer) was seen to positively correlate ($R^2 = 0.97$) with an increase in modulus (measured by rheometer) indicating the complementary nature of measurements by these instruments in determining hydrogel properties. An increase in both modulus (G' and G'') and hardness with gel concentration indicates a highly cross linked ECM structure.

Cohesivity and adhesivity were calculated from the positive and negative regions of the force-time curve, respectively. It was seen that cohesivity of the gel increased with concentration and was in the range of 4-30 g.s (Figure 6d). During the texture analyzer experiments for all concentrations, there was minimal force registered while retracting the impinging cylindrical rod. Therefore, the registered adhesivity values were low for all the gels tested and showed no particular trend. The characterization on the texture analyzer clearly show that UBM ECM gels have a more cohesive than adhesive nature at all concentrations ($p < 0.05$) indicating strong internal physico-chemical interactions within the crosslinked gel.

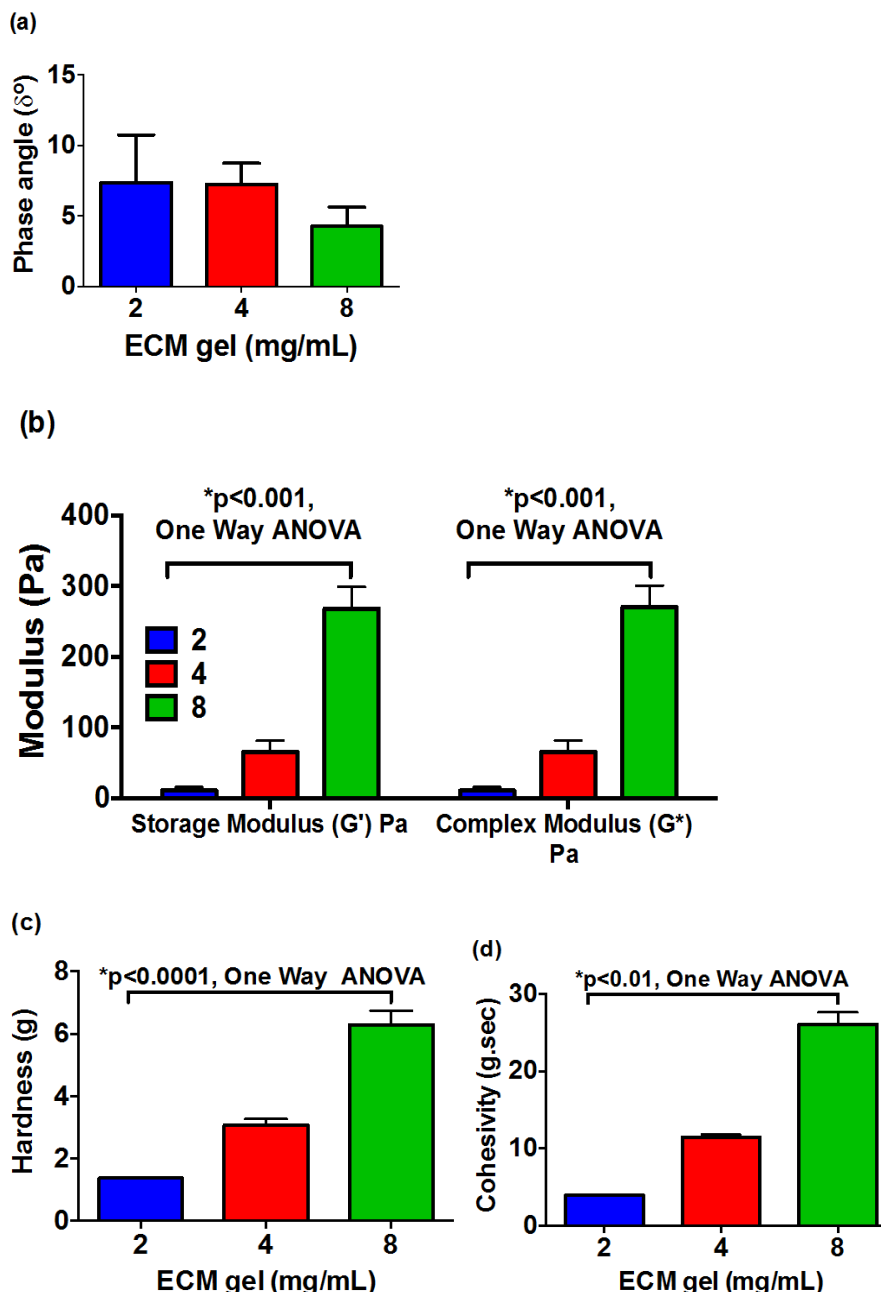


Figure 6. Hydrogel properties for 2 mg/mL (blue), 4 mg/mL (red) and 8 mg/mL (green) ($n=3$). a) Low phase angle indicating predominantly elastic gels. A concentration dependent increase was observed for b) Storage modulus (G') and complex modulus (G^*), c) Hardness, and d) Cohesivity.

Yield stress and yield strain

The rheometer was used to determine yield stress and yield strain. Yield stress is defined as the shear force required for gels to undergo permanent deformation (38) and was measured using creep studies. Creep is defined as strain or displacement experienced by a body after the application of stress. The amount of strain required for catastrophic collapse in a structure is called yield strain and was measured using the amplitude sweep. As shown in Figure 7a, yield stress increased and yield strain decreased with concentration. In other words, the gels that were able to bear higher shear forces were more prone to undergoing catastrophic collapse rather than displacement.

The decrease in yield strain with concentration was attributed to strain stiffening observed at the lower gel concentration in comparison to strain weakening observed at the higher gel concentration (Figure 7b, compare

2 and 8 mg/mL gels). Strain stiffening refers to the increase in storage modulus (G') of gels with applied strain. It is a property of biological gels such as the collagen gel that is attributed to reversible movements of the crosslinks before yielding (39). Initial stiffening is likely due to individual fiber stretching followed by network scale involving reversible fiber rearrangements. In the study by Motte et al. (40), the collagen gels showed slight strain weakening before yielding, which is similar to what was observed in our study. The 8 mg/mL gels in this study may be cross-linked to an extent that inhibits reversible movements of the crosslinks, thus reducing the strain stiffening behavior.

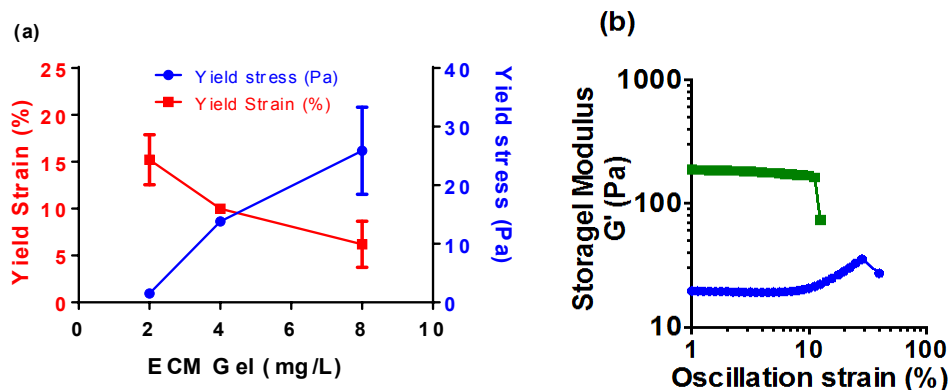


Figure 7. (n=3): a) With an increase in the ECM gel concentration, the yield stress (blue) increased and the yield strain (red) decreased. Yield stress and yield strain showed an inverse relationship with each other. b) Yield strain of 2 mg/mL (blue) and 8 mg/mL (green) ECM gels. Strain stiffening was not observed at higher ECM gel concentration.

Creep compliance

After in-situ gelation of the ECM at the site of injury, it is likely that it will experience stresses from nearby tissues. Hence, understanding the behavior of these gels under constant stress conditions is of importance. Burger's model (Equation II) describes the response of a system under stress as a sum of the elastic, visco-elastic and viscous components (41). The initial spontaneous elastic deformation is quantified by a Maxwell spring element. The intermediate visco-elastic behavior is characterized as a Kelvin-Voigt viscoelastic element (spring-dashpot parallel combination) and the viscous behavior is quantified as a dashpot viscous element. G_0 and G_1 are the elastic moduli components of the Maxwell and Kelvin-Voigt elements; η_1 and η_0 are the viscosities of Kelvin-Voigt and dashpot elements, respectively.

Burger's model equation:

$$\gamma(t) = \frac{\sigma}{G_0} + \frac{\sigma}{G_1} \left[1 - e^{-\left(\frac{t * G_1}{\eta_1}\right)} \right] + \frac{(\sigma * t)}{\eta_0} \quad (II)$$

Data from creep measurements for UBM ECM gels were fitted to Burger's model to predict the strain at different stress and time values (Figure 8) (42). The model parameters (G_0 , G_1 , η_0 , η_1) were estimated by fitting the data to the equation, and were subsequently used to evaluate the strain at different values of stress and time. Among 2, 4 and 8 mg/mL UBM ECM gels, the 2 mg/mL gels had the lowest G_0 value, which explains its greatest deformation compared to other gels. All of the Burger's model parameters increased with concentration, indicating greater opposition to deformation at higher gel concentrations (Supplementary Table 1).

While Burger's model helps estimate when permanent deformation occurs, it is important to note that it does not take into account normal stresses and degradation kinetics of the gel *in vivo*, which could impact the strain values upon prolonged stress. Previous work has shown that UBM-ECM gels degrade within 8-10 weeks of implantation *in vivo* (43). It is likely that with degradation, the Burger's model parameters would likely change due to reduced gel opposition to deformation.

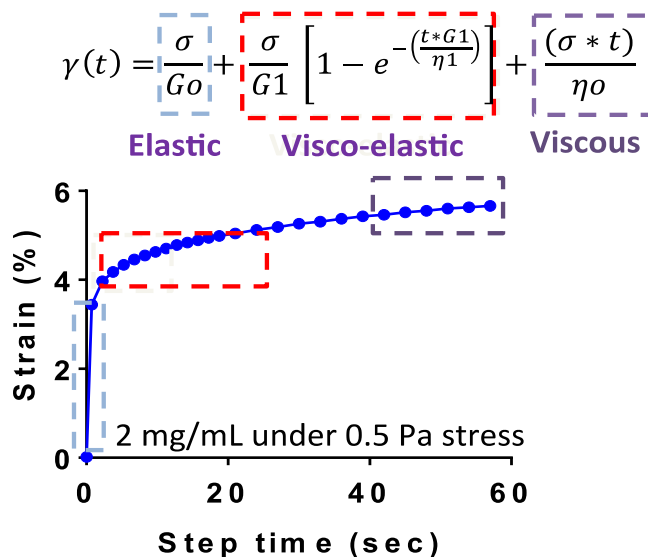


Figure 8. Creep data used to estimate Burger's model parameters. Data for 2 mg/mL UBM ECM gel obtained by applying constant stress of 0.5 Pa for 60 s shown.

Comparison of Collagen and UBM ECM Gels

Collagen has already been shown to be the major component of ECM gels (6). However, there are other structural and functional proteins and peptides (proteoglycans, sulfated GAGs, and fibronectin, etc.) that differentiate the ECM gels from collagen gels. It is of importance to study the impact the other proteins (apart from collagen) have on the different mechanical properties of ECM gels. As seen in Supplementary Figure 1, ECM pre-gel showed lower viscosity compared to the collagen pre-gel solutions. Similar to the ECM pre-gel solution, collagen also showed a concentration dependent increase in viscosity.

With regard to gelation kinetics, UBM ECM gels showed no impact of concentration on gelation time between 2 to 8 mg/mL (Figure 5d). On the other hand, an increase in collagen monomer concentration from 2 to 8 mg/mL resulted in a decrease in gelation time from 14 to 8 min (Supplementary Figure 2). This is due to the higher concentration of monomers in the collagen matrix, which translates into lower diffusion time scales and faster gelation. This observation is confirmed in literature (37). It was also observed that at every concentration, UBM ECM gels showed significantly faster gelation time than collagen gels ($p < 0.05$) (Supplementary Figure 2). In UBM ECM gels, soluble proteoglycans and sulfated GAGs can electrostatically associate with collagen fibrils and impact their nucleation and growth leading to the reduction of gelation time (35).

The collagen gels showed higher modulus, hardness, cohesivity and adhesivity compared to UBM ECM at all concentrations studied, as shown in Supplementary Figure 3. Similar to ECM gels, the collagen gels were found to have significantly more cohesivity compared to adhesivity albeit significantly higher values for both of these texture properties compared to the ECM gels. Guarnieri et al (44) showed that the presence of components such as fibronectin and laminin in the collagen gels can be attributed to weaker and looser cross-links, with a significant decrease in storage and loss moduli at a concentration of 100 $\mu\text{g/mL}$. It is likely that the complex mixture of components in ECM gels decrease the storage and loss moduli, and the texture properties.

The collagen gels showed similar levels of yield stress compared to UBM ECM gels but had significantly higher yield strain (%) at 4 and 8 mg/mL (Supplementary Figure 4). Though the ECM gels show lower hardness than the collagen gels, similar yield stress and lower yield strain values indicate that the ECM gels would be able to resist similar amounts of shear stress compared to the collagen gels. The non-structural components in the ECM might influence yield stress values and allow them to be equivalent to that of collagen.

The collagen gels at all concentrations showed strain stiffening behavior (Supplementary Figure 5), unlike the ECM gels that did not show strain stiffening at 8 mg/mL (Figure 7b). It is likely that the inclusion of soluble proteoglycans and sGAGs lower the ability of ECM gels to undergo strain stiffening by preventing the reversible movements of the crosslinks. In addition, collagen gels showed a significantly greater extent of strain stiffening compared to UBM ECM gels at all concentrations ($p < 0.05$, unpaired t-test)

Supplementary Table 1 shows the Burger's model fit of creep under constant stress for UBM ECM and collagen gels. It was broadly seen that all the model parameters were higher for collagen gels compared to the UBM ECM gels. Higher G_0 and G_1 values indicate that the collagen gels show greater opposition to deformation compared to UBM ECM gels. Overall, the UBM ECM gels were found to be weaker than collagen gels likely due to different protein fractions present within the ECM gels that inhibit fibril formation.

Drug Loading in to the ECM Gels: Impact on Gelation Kinetics and Complex Modulus

Inclusion of a small molecule drug compound into the ECM gels could augment regenerative capabilities. One of the ways to incorporate small molecule drugs into the gel is to trap the drug nanoparticles within the network of the gel. To test the hypothesis that incorporation of drug molecules into the gel would likely disturb its network and impact its mechanical properties, the rheological response of UBM ECM gels following drug loading was studied. Two model drugs were incorporated into 4 mg/mL UBM ECM gels. These drugs were selected based on charge at neutral pH: glipizide is negative and tamsulosin is positive at neutral pH. It was hypothesized that the charge of the drug molecules might affect the formation of the gel network in different ways. The impact of drug load (25 or 50 wt%/wt%) was also investigated.

The gelation time for drug-loaded gels (Figure 9) was determined using the same method as for the native gels. Presence of the drugs did not impact the gelation time compared to the control. An increase in drug load from 25 to 50 wt%/wt% also did not affect gelation time. The results were tested for statistical significance using the Tukey-Kramer test and were found to have no statistical significance.

Incorporation of the drugs did affect the complex modulus of the gels (Figure 10a). The glipizide-loaded gels had a complex modulus that was significantly lower than that of the control at both drug loads. Additionally, complex modulus decreased as the drug load increased for glipizide. On the other hand, tamsulosin showed the opposite effect in response to the drug load. Complex modulus for the tamsulosin-loaded gel was slightly lower (not statistically significant) than the control at 25 wt%/wt% drug loads, but similar to the control at 50 wt%/wt% drug load.

Complex modulus is described by elastic and viscous components through the storage (Figure 10b) and loss moduli (Figure 10c), respectively. Since the storage and complex moduli followed the same trend, it can be concluded that only elastic properties of the gels were affected by drug incorporation.

Glipizide in the gels is negatively charged, and a reduction in storage and/or complex modulus with an increase in the drug load indicates that the gels are less stable in the presence of the drug. The tamsulosin-loaded gels undergo less of a change at either drug load, indicating higher stability. The results indicate that the UBM ECM gels would be more mechanically robust with positively charged drugs such as tamsulosin. For negatively charged drugs an additional component may be required to maintain the gel properties.

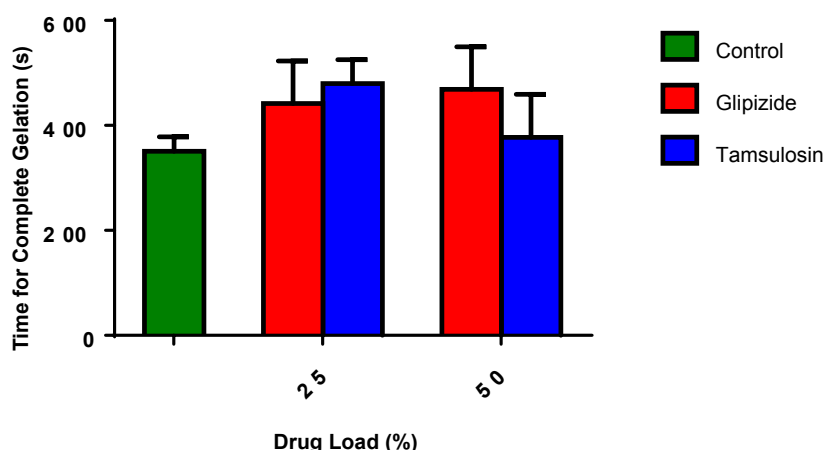


Figure 9. Effect of drug loading on gelation time for 4 mg/mL ECM gels ($n=2$). No statistically significant differences between control, naïve gel (green), glipizide-loaded (red) and tamsulosin-loaded (blue) gels was observed.

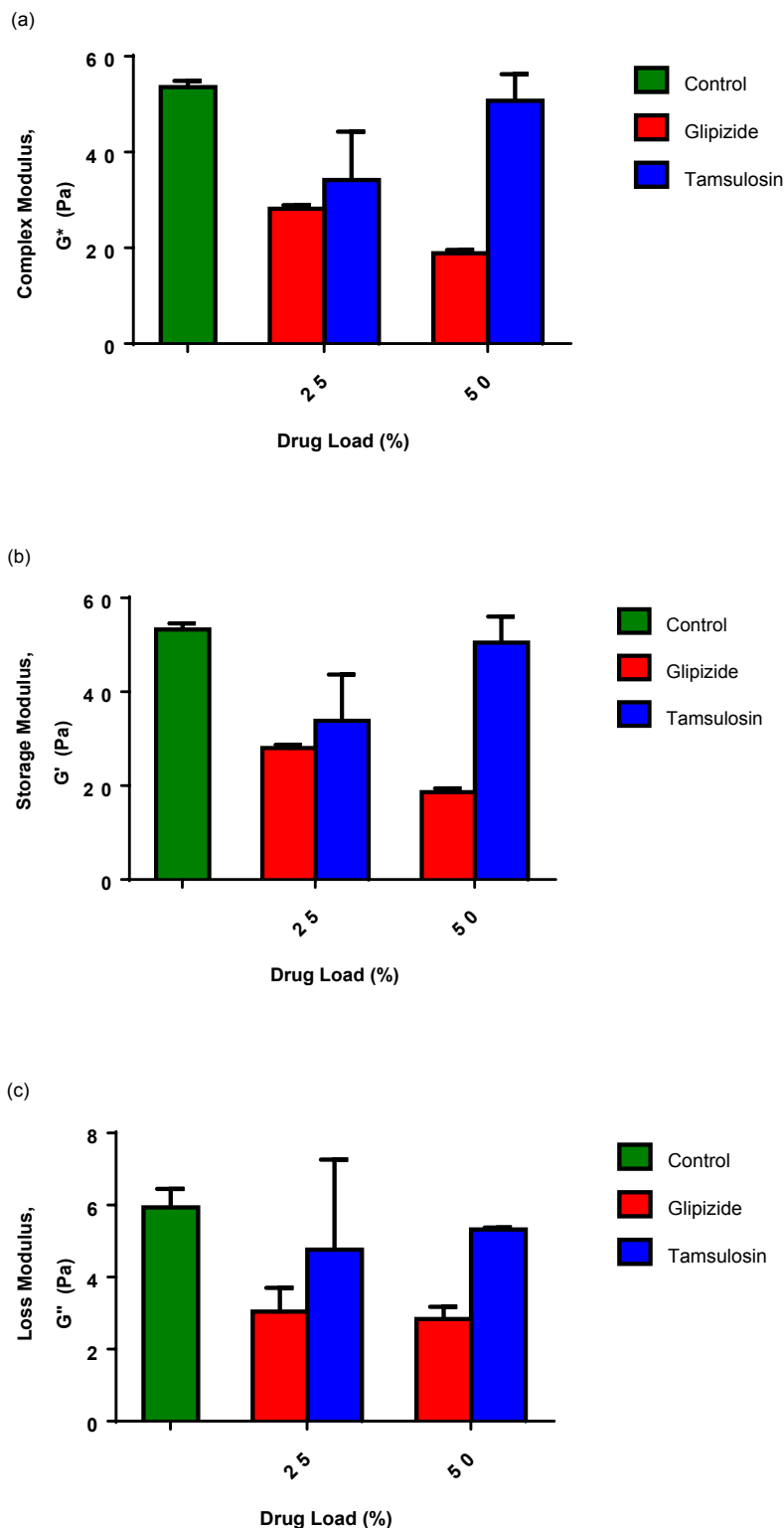


Figure 10. a) Complex, b) storage, and c) loss modulus of 4 mg/mL ECM gels with 0, 25 or 50 wt%/wt% drug load (n=2).

CONCLUSION

This study provides a detailed mechanical assessment of viscoelastic properties of UBM ECM gels by rheometer and texture analyzer. The tests were conducted for various stages of hydrogel formation in order to understand nuances of the system behavior as a function of its stages and to aid in proper handling for in vivo studies. The study was conducted for specific UBM hydrogel and corresponding studies should be done for the select systems. We determined that:

- For all concentrations of UBM ECM gels, rapid gelation was observed around 25°C with a gel point of less than 5 min.
- Gel complex modulus measured using rheometer correlated with hardness measured using texture analyzer, indicating that the measurements done with rheometer and texture analyzer were complementary to each other.
- Yield stress and yield strain were negatively correlated and gels were found to undergo strain stiffening at lower concentrations.
- The collagen gels in comparison to the UBM ECM gels had higher pre-gel viscosity, modulus, hardness and gelation time. The collagen gels also showed a greater degree of strain stiffening than the UBM ECM gels.
- Insoluble drugs were loaded into the UBM ECM gels, and impacted the mechanical properties of the gels depending on the charge of the drug.

Although, a specific hydrogel UBM system was used in this study the recommendation to utilize both techniques due to their complementary nature can be extended to other hydrogel systems. This would yield a more comprehensive understanding of mechanical properties of systems and would allow for better development decisions.

ACKNOWLEDGEMENT

We thank Vertex Pharmaceuticals Incorporated for funding this research work. We would like to thank Dr. Stephen Badylak's group at McGowan Institute of Regenerative Medicine, University of Pittsburgh for their expertise with ECM gels and also for supplying the UBM ECM used in this study. We would also like to thank TA instruments and Texture Technologies for their technical support with the rheometer and the texture analyzer, respectively.

REFERENCES

1. Kashyap N, Kumar N, Kumar M, Hydrogels for pharmaceutical and biomedical applications, Crit Rev Ther Drug Carrier Syst, 22(2); 107-49, 2005.
2. Slaughter B, Khurshid S, Fisher O, Khademhosseini A, Peppas N, Hydrogels in regenerative medicine, Adv Mater, 21(32-33); 3307-3329, 2009.
3. Yang J, Yeom J, Hwang B, Hoffman A, Hahn S, *In situ*-forming injectable hydrogels for regenerative medicine, Progr Polym Sci, 39(12); 1973-1986, 2014.
4. Prestwich G, Hyaluronic acid-based clinical biomaterials derived for cell and molecule delivery in regenerative medicine, J Control Release, 155(2); 193-199, 2011.
5. Medberry CJ, Crapo PM, Siu BF, Carruthers CA, Wolf MT, Nagarkar SP, Agrawal V, Jones KE, Kelly J, Johnson SA, Velankar SS, Watkins SC, Modo M, Badylak SF, Hydrogels derived from central nervous system extracellular matrix, Biomaterials, 34(4); 1033-1040, 2013.
6. Freytes D, Martin J, Velankar S, Lee A, Badylak S, Preparation and rheological characterization of a gel form of the porcine urinary bladder matrix, Biomaterials, 29(11); 1630-1637, 2008.
7. Dao M, Hashino K, Kato I, Nolte J, Adhesion to fibronectin maintains regenerative capacity during *ex vivo* culture and transduction of human hematopoietic stem and progenitor cells, Blood, 92(12); 4612-4621, 1998.
8. Rooney J, Gurpur P, Yablonka-Reuveni Z, Burkin D, Laminin-111 restores regenerative capacity in a mouse model for $\alpha 7$ integrin congenital myopathy, Am J Pathol, 174(1); 256-264, 2009.
9. Geiger M, Li R, Friess W, Collagen sponges for bone regeneration with rhBMP-2, Adv Drug Deliv Rev, 55(12); 1613-29, 2003.
10. Frantz C, Stewart K, Weaver V, The extracellular matrix at a glance, J Cell Sci, 123(24); 4195-4200, 2010.
11. Busch S, Silver J, The role of extracellular matrix in CNS regeneration, Curr Opin Neurobiol, 17(1); 120-127, 2007.

12. Barros C, Franco S, Müller U, Extracellular matrix: functions in the nervous system, *Cold Spring Harb Perspect Biol*, 3(1); a005108, 2011.
13. Fawcett J, The extracellular matrix in plasticity and regeneration after CNS injury and neurodegenerative disease, *Prog Brain Res*, 218; 213-226, 2015.
14. Wolf MT, Daly KA, Brennan Pierce EP, Johnson SA, Carruthers CA, Amore A, Nagarkar SP, Velankar SS, Badylak SF, A hydrogel derived from de-cellularized dermal extracellular matrix, *Biomaterials*, 33(29); 7028-7038, 2012.
15. Badylak SF, Kochupura PV, Cohen IS, Doronin SV, Saltman AE, Gilbert TW, Kelly DJ, Ignatz RA, Gaudette GR, The use of extracellular matrix as an inductive scaffold for the partial replacement of functional myocardium, *Cell Transplant*, 15; 29-40, 2016.
16. Kimmel H, Rahn M, Gilbert T, The clinical effectiveness in wound healing with extracellular matrix derived from porcine urinary bladder matrix: A case series on severe chronic wounds, *J Am Col Certif Wound Spec*, 2(3): 55-9, 2010.
17. Afaneh C, Abelson J, Schattner M, Janjigian YY, Ilson D, Yoon SS, Strong VE, Esophageal reinforcement with an extracellular scaffold during total gastrectomy for gastric cancer, *Ann Surg Oncol*, 22(4); 1252-1257, 2015.
18. Parcels A, Abernathie B, Datiashvili R, The use of urinary bladder matrix in the treatment of complicated open wounds, *Wounds*, 26(7); 189-196, 2014.
19. Wang J, Thampatty B, An introductory review of cell mechanobiology. *Biomech Model Mechanobiol*, 5(1); 1-16, 2006.
20. Badylak S, Freytes D, Gilbert T, Extracellular matrix as a biological scaffold material: Structure and function, *Acta Biomater*, 5(1); 1-13, 2009.
21. Li X, Katsanevakis E, Liu X, Zhang N, Wen X, Engineering neural stem cell fates with hydrogel design for central nervous system regeneration, *Prog Polym Sci*, 37(8); 1105-1129, 2015.
22. Saha K, Keung AJ, Irwin EF, Li Y, Little L, Schaffer DV, Healy KE, Substrate modulus directs neural stem cell behavior, *Biophys J*, 95(9); 4426-4438, 2008.
23. Ghuman H, Massensini AR, Donnelly J, Kim SM, Medberry CJ, Badylak SF, Modo M, ECM hydrogel for the treatment of stroke: Characterization of the host cell infiltrate, *Biomaterials*, 91; 166-181, 2016.
24. Klaas M, Kangur T, Viil J, Mäemets-Allas K, Minajeva A, Vadi K, Antsov M, Lapidus N, Järvekülg M, Jaks V, The alterations in the extracellular matrix composition guide the repair of damaged liver tissue, *Sci Rep*, 6(6); 27398, 2016.
25. Baker E, Bonnecaze R, Zaman M, Extracellular matrix stiffness and architecture govern intracellular rheology in cancer, *Biophys J*, 97(4); 1013-1021, 2009.
26. Ulrich T, Jain A, Tanner K, MacKay J, Kumar S, Probing cellular mechanobiology in three-dimensional culture with collagen-agarose matrices, *Biomaterials*, 31(7); 1875-1884, 2010.
27. Instructions for TA HR-2 Shear Rheometer.
28. Engler A, Bacakova L, Newman C, Hategan A, Griffin M, Discher D, Substrate compliance versus ligand density in cell on gel responses, *Biophys J*, 86(1); 617-628, 2004.
29. Ehrbar M, Sala A, Lienemann P, Ranga A, Mosiewicz K, Bittermann A, Rizzi SC, Weber FE, Lutolf MP, Elucidating the role of matrix stiffness in 3D cell migration and remodeling, *Biophys J*, 100(2); 284-293, 2011.
30. Cheng G, Tse J, Jain R, Munn L, Micro-environmental mechanical stress controls tumor spheroid size and morphology by suppressing proliferation and inducing apoptosis in cancer cells, *PLoS One*, 4(2); e4632, 2009.
31. Engler A, Sen S, Sweeney H, Discher D, Matrix elasticity directs stem cell lineage specification, *Cell*, 126(4), 677-689, 2006.
32. Yan C, Altunbas A, Yucel T, Nagarkar R, Schneider J, Pochan D, Injectable solid hydrogel: Mechanism of shear-thinning and immediate recovery of injectable β -hairpin peptide hydrogels, *Soft Matter*, 6(20); 5143-5156, 2010.

33. Liang Y, Walczak P, Bulte J, The survival of engrafted neural stem cells within hyaluronic acid hydrogels, *Biomaterials*, 34(22); 5521-5529, 2013.
34. Li Y, The mechanism of collagen self-assembly: Hydrophobic and electrostatic interactions, Thesis, University of Florida, 2009.
35. Oegema T, Laidlaw J, Hascall V, Dziwiatkowski D, The effect of proteoglycans on the formation of fibrils from collagen solutions, *Arch Biochem Biophys*, 170(2); 698-709, 1975.
36. Ruggeri A, Benazzo F, Collagen-proteoglycan interaction, *Ultrastructure of the Connective Tissue Matrix*, Springer US, 113-25, 1984.
37. Yang Y, Kaufman L, Rheology and confocal reflectance microscopy as probes of mechanical properties and structure during collagen and collagen/hyaluronan self-assembly, *Biophys J*, 96(4); 1566-1585, 2009.
38. Buehler M, Nanomechanics of collagen fibrils under varying cross-link densities: atomistic and continuum studies, *J Mech Behav Biomed Mater*, 1(1); 59-67, 2008.
39. Arevalo R, Urbach J, Blair D, Size-dependent rheology of type-I collagen networks, *Biophys J*, 99(8); L65-L7, 2010.
40. Motte S, Kaufman L, Strain stiffening in collagen I networks, *Biopolymers*, 99(1); 35-46, 2013.
41. Dolz M, Hernández M, Delegido J, Creep and recovery experimental investigation of low oil content food emulsions, *Food Hydrocoll*, 22(3); 421-7, 2008.
42. Martucci J, Ruseckaite R, Vazquez A, Creep of glutaraldehyde-crosslinked gelatin films, *Mater Sci Eng*, 435; 681-686, 2006.
43. Valentin J, Stewart-Akers A, Gilbert T, Badylak S, Macrophage participation in the degradation and remodeling of extracellular matrix scaffolds, *Tissue Eng Part A*, 15(7); 1687-1694, 2009.
44. Guarnieri D, Battista S, Borzacchiello A, Mayol L, De Rosa E, Keene DR, Muscariello L, Barbarisi A, Netti PA, Effects of fibronectin and laminin on structural, mechanical and transport properties of 3D collageneous network, *J Sci Mater Med*, 18(2); 245-53, 2007.